

Slow dynamics of nonequilibrium density fluctuations in hard-sphere suspensions

Michio Tokuyama,^{1,*} Yoshihisa Enomoto,² and Irwin Oppenheim¹

¹*Department of Chemistry, Massachusetts Institute of Technology, Cambridge, Massachusetts 02139*

²*Department of Physics, Nagoya Institute of Technology, Nagoya 466, Japan*

(Received 6 August 1996)

The coupled diffusion equations recently proposed for concentrated hard-sphere suspensions are numerically solved to investigate the dynamics of density fluctuations around time-dependent nonequilibrium (spatially inhomogeneous) states. As the volume fraction of spheres ϕ approaches the critical value ϕ_g from below, the self-intermediate scattering function $F_S(\mathbf{k}, t)$ is shown to obey two different slow relaxations whose time scales t_β and t_α diverge as the separation parameter $\sigma = (\phi - \phi_g)/\phi_g$ approaches zero: $t_\beta \sim |\sigma|^{-\beta}$ and $t_\alpha \sim |\sigma|^{-\alpha}$, where $\phi_g = (4/3)^3 / (7 \ln 3 - 8 \ln 2 + 2)$. Thus, the importance of nonequilibrium effects on slow dynamics is stressed from a unifying viewpoint. [S1063-651X(97)50601-5]

PACS number(s): 82.70.Dd, 05.40.+j, 51.10.+y

Recent experimental works [1–3] show that concentrated hard-sphere suspensions also exhibit a transition from a fluids phase to a glass phase, similar to that in supercooled liquids. Many attempts to understand the dynamics of suspensions approaching the glass transition have been made by employing the mode-coupling theory (MCT) [4,5] for the dynamics of supercooled fluids. The most striking feature of MCT is the prediction of two different slow relaxations of density fluctuations, the so-called β and α relaxations, whose time scales t_β and t_α are singular as $t_\beta \sim |1 - \phi/\phi_c|^{-\beta}$ and $t_\alpha \sim |1 - \phi/\phi_c|^{-\alpha}$, where ϕ_c is a critical packing fraction, and α and β are exponents to be determined. In concentrated colloidal suspensions [2–4], MCT predicts $\beta=1.66$ and $\alpha=2.58$. Thus, MCT has stimulated much of the recent experiment, computational and theoretical works on colloidal suspensions. In this paper, we present a theoretical approach different from MCT in the following three basic view points. First, MCT has been applied mainly to equilibrium systems. On the other hand, the present theory deals with a nonequilibrium system and starts with the nonlinear deterministic diffusion equation for the average number density $n(\mathbf{x}, t)$, which was recently derived by Tokuyama and Oppenheim on the time scale much longer than the Brownian relaxation time t_B [6]. This is because most experimental measurements are, in general, done in quenched metastable fluid states prior to crystallization where the nonequilibrium effects may change the behavior of relaxation processes. The deterministic equation for $n(\mathbf{x}, t)$ then describes the nonequilibrium transitional behavior from a nonequilibrium initial state with $n(\mathbf{x}, 0)$ to an equilibrium state with $n(\mathbf{x}, \infty) = n_0$, where $n_0 = N/V$ is the equilibrium number density, N and V being the total number of Brownian particles and the total volume of the system, respectively. Second, MCT assumes that the density fluctuations obey the nonlinear stochastic equations for the density fluctuations $\delta n(\mathbf{x}, t)$. On the other hand, the present theory starts with the linear stochastic diffusion equation for the density fluctuations $\delta n(\mathbf{x}, t)$ recently pro-

posed by Tokuyama [7], which describes a linear relaxation around the time-dependent nonequilibrium state. This is because the density fluctuations should be small compared to the average number density, since the glass transition seems not to be a critical phenomenon. In fact, the glass transition is dynamic in origin in contrast to critical phenomena, and hence, there is no correlation length diverging at the glass transition point. Finally, in hard-sphere suspensions MCT contains two parameters, the volume fraction of particles ϕ , and a microscopic time scale τ_0 which is treated as a free fit parameter. On the other hand, the present theory contains two parameters, ϕ and the initial number density $n(\mathbf{x}, 0)$, both of which can be fixed by an experiment.

Recently, the above coupled diffusion equations were investigated asymptotically [7] and analytically [8]. Thus, the two different slow relaxations with the exponents $\beta=1$ and $\alpha=2$ were predicted to exist near the critical volume fraction $\phi_g \approx 0.571847\dots$, if the system is initially nonequilibrium. In this paper, therefore, we numerically solve those coupled diffusion equations self-consistently under appropriate initial conditions and thus investigate the dependence of the slow dynamics on the two parameters, ϕ and $n(\mathbf{x}, 0)$, including the temporal power laws and the crossovers.

The particle dynamics of colloidal suspensions can be measured by dynamic light scattering through the intermediate scattering function [9], which is given by the Fourier transform $F(\mathbf{k}, t)$ of the autocorrelation function of the density fluctuations $F(\mathbf{x}, t) = \langle \delta n(\mathbf{x}, t) \delta n(\mathbf{0}, 0) \rangle / N$, where the angular brackets denote the average over the canonical ensemble. The scattering function $F(\mathbf{k}, t)$ can be separated into a self-part $F_S(\mathbf{k}, t)$, which describes the average self-motion of individual particles, and a cross-part $F_C(\mathbf{k}, t)$, which describes the average relative motion between different particles: $F(\mathbf{k}, t) = F_S(\mathbf{k}, t) + F_C(\mathbf{k}, t)$. Since in the present work we are interested only in scattering vectors much larger than the maximum position k_m of the structure factor $S(\mathbf{k}) = F(\mathbf{k}, 0)$, we can neglect the cross-part $F_C(\mathbf{k}, t)$. Introducing the Fourier transform of $n(\mathbf{x}, t)$ by $n_k(t) = \int d\mathbf{x} \exp(i\mathbf{k} \cdot \mathbf{x}) n(\mathbf{x}, t)$, therefore, we start with the coupled diffusion equations for $n_k(t)$ and $F_S(\mathbf{k}, t)$ [6–8]

*Permanent address: Statistical Physics Division, Tohwa Institute for Science, Tohwa University, Fukuoka 815, Japan.

$$\frac{\partial}{\partial t} n_k(t) = -k^2 D_S^L(\phi) n_k(t) - D_S^S(\phi) \sum_q \mathbf{k} \cdot \mathbf{q} M_{k-q}(t) n_q(t), \quad (1)$$

$$\frac{\partial}{\partial t} F_S(\mathbf{k}, t) = -k^2 D_S^L(\phi) F_S(\mathbf{k}, t) - k^2 D_S^S(\phi) \sum_q M_{k-q}(t) F_S(\mathbf{q}, t), \quad (2)$$

with the Fourier transform $M_k(t)$ of the memory function

$$M(z(\mathbf{x}, t)) = \frac{(1-z)[\hat{D}_S^S(1-\hat{\phi}^2 z) + u\{\hat{D}_S^S \hat{\phi}^2 z(-1+\hat{\phi} z + \sigma) + \sigma^2(1-\hat{\phi} z)^2\}]}{V(\hat{D}_S^S + \sigma^2/\hat{\phi})[\hat{D}_S^S \hat{\phi} z + (1-\hat{\phi} z)^2]}, \quad (3)$$

where $z(\mathbf{x}, t) = n(\mathbf{x}, t)/n_0$, $\hat{D}_S^S = D_S^S/D_0$, $\phi = 4\pi a_0^3 n_0/3$, $\hat{\phi} = \phi/\phi_g$, and $\sigma = \hat{\phi} - 1$, D_0 and a_0 being the single-particle diffusion coefficient and the particle radius, respectively. Here $D_S^S(\phi)$ and $D_S^L(\phi)$ denote the short- and the long-time self-diffusion coefficient, respectively (see Ref. [6] for details). The coupling factor $u = (9/32)\phi_g$ denotes the coupled effect between the many-body short-range hydrodynamic interactions and the many-body direct interactions among particles. The long-time self-diffusion coefficient D_S^L and the memory function $M(z)$ can be written, near ϕ_g , as

$$D_S^L \sim D_0(1-u)\sigma^2 + O(\sigma^3), \quad (4)$$

$$M(z) \sim -2\sigma(1-z)\{(1-u)/\hat{D}_S^S\} + O(\sigma^2(1-z)^2).$$

We should mention here that these properties result from the correlation effects due to the many-body long-range hydrodynamic interactions between particles [6], leading to the two different slow relaxations [7,8].

Equation (1) is the nonlinear diffusion equation for $n_k(t)$ and describes a transient behavior of the average number density $n_k(t)$ from a spatially inhomogeneous, nonequilibrium initial state described by $n_k(0)$ to the spatially homogeneous, equilibrium state given by $n_0 \delta_{\mathbf{k},0}$ under the conservation law $n_0(t) = n_0$. We should note here that the memory function $M(z(\mathbf{x}, t))$ describes the nonequilibrium effect. In fact, it becomes zero in the equilibrium state where $z(\mathbf{x}, t) = 1$. Thus, the diffusion field (or the relaxation time) changes in space and time if the initial state of the system is nonequilibrium.

Equation (2) is the linear diffusion equation for $F_S(\mathbf{k}, t)$ which describes a linear relaxation of the self-diffusion process around the time-dependent nonequilibrium states determined by Eq. (1). Solving it formally, we obtain

$$F_S(\mathbf{k}, t) = f(\mathbf{k}, t; \phi) \exp(-k^2 D_S^L t) \quad (5)$$

with the memory part

$$f(\mathbf{k}, t; \phi) = [\exp_{-}\{-\mathbf{m}(t; \phi)\}]_{kk}, \quad (6)$$

where $\mathbf{m}(t; \phi)$ denotes the matrix whose (\mathbf{k}, \mathbf{q}) component is given by

$$m_{kq}(t; \phi) = \int_0^t \exp(k^2 D_S^L s) \{k^2 D_S^S M_{k-q}(s)\} \times \exp(-q^2 D_S^L s) ds \quad (7)$$

Here \exp_{-} denotes a time-ordered exponential, ordered from the left. Thus, the scattering function $F_S(\mathbf{k}, t)$ is factorized into a memory part, which depends on the initial conditions for $n_k(0)$, and a long-time part, which is independent of such initial conditions.

For the short-time region of order $t_\gamma = 2\pi/k^2 D_S^S$, the relaxation obeys the short-time decay $F_S^S(\mathbf{k}, t) = [\exp_{-}\{-\dot{\mathbf{m}}(0; \phi)t\}]_{kk}$, which is mainly governed by the

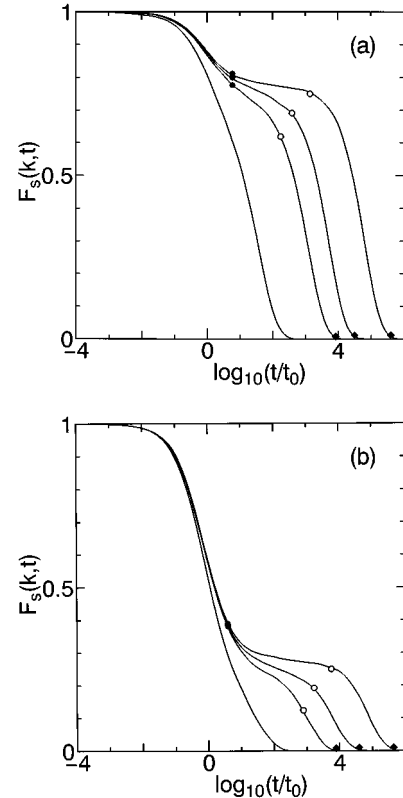


FIG. 1. Self-intermediate scattering function $F_S(\mathbf{k}, t)$ vs $\log(t/t_0)$ at (a) $z_0 = 0.8$ and (b) $z_0 = 0.5$ for different volume fractions (from left to right): 0.543, 0.566, 0.569, and 0.571, where $ka_0 = 2.8$ and $t_0 = a_0^2/D_0$. The symbols indicate the time scales: t_β (\bullet), t_α (\circ), and t_α (\blacklozenge).

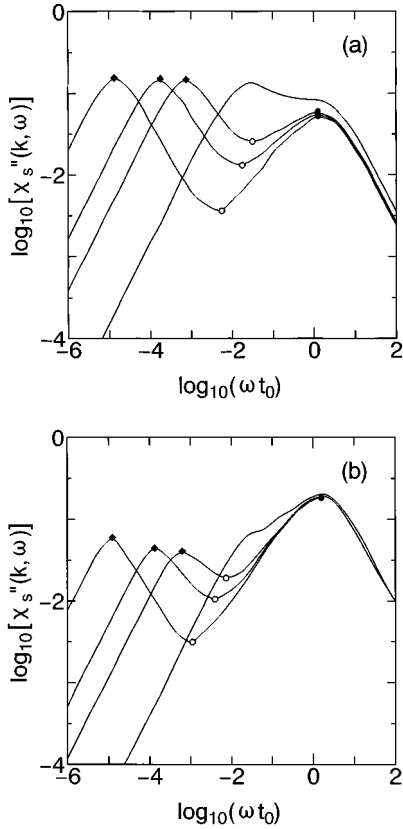


FIG. 2. Log-log plot of self-part of dynamic susceptibility $\chi''_S(\mathbf{k}, \omega)$ vs ωt_0 for different volume fractions (from left to right): 0.571, 0.569, 0.566, and 0.543. Details are the same as in Fig. 1. The symbols indicate the frequencies: ω_γ (●), ω_β (○), and ω_α (◆).

short-time self-diffusion coefficient D_S^S . On the other hand, for the long-time region of order $t_\alpha = 2\pi/k^2 D_S^L$, we have $n(\mathbf{x}, t) = n_0$ and $M(z(\mathbf{x}, t)) = 0$. Hence, the relaxation is described by the long-time decay $F_S^L(\mathbf{k}, t) = \exp(-k^2 D_S^L t)$. Thus, there exists a crossover from the short-time relaxation process to the long-time relaxation process.

For the intermediate-time region $t_\gamma \ll t \ll t_\alpha$, the dynamical behavior of $F_S(\mathbf{k}, t)$ becomes more complicated because of the memory function $M(z(\mathbf{x}, t))$, which causes a structural arrest. In fact, near ϕ_g , the number density $n(\mathbf{x}, t)$ is expected to become almost n_0 after some time t_e between t_γ and t_α [7,8]. Since $M(z(\mathbf{x}, t))$ reduces to zero for $t \geq t_e$, Eq. (5) can be approximately written as $F_S(\mathbf{k}, t) \approx f(\mathbf{k}, t_e; \phi) \exp(-k^2 D_S^L t)$. For intermediate times $t_e \leq t \ll t_\alpha$, therefore, $F_S(\mathbf{k}, t)$ becomes nearly constant for a while, since $k^2 D_S^L t \ll 1$. This continues up to the time t_β where the term $k^2 D_S^L t$ becomes the same order as the term $\mathbf{m}(t_e; \phi)$. On the time scale of order t_β , $F_S(\mathbf{k}, t)$ then starts to decay again, obeying $F_S^L(\mathbf{k}, t)$. Thus, t_β denotes the crossover time from structural arrest to long-time decay and is found, using Eq. (4), as $t_\beta \sim |\sigma|^{-1}$, $t_e \ll t_\beta \ll t_\alpha$. Near ϕ_g , the nonequilibrium effect is thus expected to cause two different slow relaxations, the so-called β and α relaxations, with the time scales $t_\beta \sim |\sigma|^{-1}$ and $t_\alpha \sim |\sigma|^{-2}$.

We now solve the coupled diffusion equations (1) and (2) self-consistently under appropriate initial conditions and investigate the self-intermediate scattering function $F_S(\mathbf{k}, t)$

TABLE I. Time exponents b_0 and b for different values z_0 and ϕ at $ka_0 = 2.8$.

ϕ	$z_0 = 0.5$		$z_0 = 0.8$	
	b_0	b	b_0	b
0.566	0.41	0.42	0.46	0.61
0.569	0.38	0.54	0.42	0.68
0.571	0.31	0.66	0.34	0.74

and the self-part of the dynamic susceptibility given by $\chi''_S(\mathbf{k}, \omega) = \omega \int_0^\infty \cos(\omega t) F_S(\mathbf{k}, t) dt$ numerically. To intergrate those equations, we employ the forward Euler difference scheme with the time step $0.01 a_0^2 / D_0$ and the lattice spacing $0.5 a_0$ in the volume $(128 a_0)^3$ of the simulation system. As the initial conditions, we fix the values of the particle volume fraction ϕ and the reduced initial number density $z(\mathbf{x}, 0) = n(\mathbf{x}, 0) / n_0$. In order to distinguish the initial states from each other qualitatively, it is convenient to introduce a parameter z_0 , which measures how close the initial state of the system is to the equilibrium state and is given by

$$z_0 = 1 - \frac{1}{V} \int d\mathbf{x} |1 - z(\mathbf{x}, 0)|, \quad (8)$$

where $0 \leq z_0 \leq 1$, and $z_0 = 1$ in equilibrium. Then, the initial value $z(\mathbf{x}, 0)$ is chosen at each position \mathbf{x} from a random number with a Gaussian distribution, which is characterized by a mean value 1 and a standard deviation S . Here the standard deviation s is adjusted so as to satisfy Eq. (8) for a given value z_0 . In the following, we thus discuss the numerical results for two typical states: (a) a near-equilibrium state with $z_0 = 0.8$, where $s = 0.235$, and (b) a nonequilibrium state with $z_0 = 0.5$, where $s = 0.591$.

In Figs. 1(a) and 1(b) we show the time evolution of $F_S(\mathbf{k}, t)$ at (a) $z_0 = 0.8$ and (b) $z_0 = 0.5$ for various volume fractions where $ka_0 = 2.8$. For small volume fractions where $t_\beta \leq t_e$, the scattering function decays quickly to zero. As the volume fraction increases and t_β becomes larger than t_e , the shape of the scattering functions becomes very sensitive to the volume fraction, forming a shoulder, which becomes at ϕ_g a plateau with the height [7,8]

$$f_k^c(z_0) = \lim_{t \rightarrow \infty} F_S(\mathbf{k}, t) = \lim_{t \rightarrow \infty} f(\mathbf{k}, t; \phi_g). \quad (9)$$

In order to see the crossover behavior in the intermediate-time region more clearly, we also calculate the self-part of the dynamic susceptibility $\chi''_S(\mathbf{k}, \omega)$. In Figs. 2(a) and 2(b) we plot it at (a) $z_0 = 0.8$ and (b) $z_0 = 0.5$ for different volume fractions where $ka_0 = 2.8$. There are two peaks and one minimum in $\chi''_S(\mathbf{k}, \omega)$. The first peak is the so-called α peak at $\omega = \omega_\alpha$ in the lower-frequency region and describes the long-time relaxation process on the time scale of order t_α . The second peak is the so-called β peak at $\omega = \omega_\beta$ in the higher-frequency region and describes the short-time relaxation process on the time scale of order t_γ . The minimum at the frequency $\omega = \omega_\beta$ corresponds to the crossover point in $F_S(\mathbf{k}, t)$ at the time t_β , where $\omega_\alpha \ll \omega_\beta \ll \omega_\gamma$. Then, the characteristic frequencies ω_α , ω_β , and ω_γ are related to the

characteristic times t_α , t_β , and t_γ through $\omega_i t_i = 2\pi$ ($i = \alpha, \beta, \gamma$), and are shown to be scaled with the separation parameter σ as

$$\omega_\alpha \sim |\sigma|^\alpha, \quad \omega_\beta \sim |\sigma|^\beta, \quad \omega_\gamma \sim |\sigma|^\gamma, \quad (10)$$

where $\alpha=2.03$ (a) and 1.99 (b), and $\beta=0.97$ (a) and 1.02 (b). Thus, the analytical values $\alpha=2$ and $\beta=1$ predicted previously in Ref. [8] are numerically verified to hold.

From Figs. 1 and 2, we see that the plateau height in the near-equilibrium state (a) is higher than that in the nonequilibrium state (b), and the α peak in (a) is higher than that in (b), while the β peak in (a) is lower than that in (b). This is because the memory function $M(z(\mathbf{x}, t))$ in (b) is much larger than that in (a) since in (b) it takes a longer time for $n(\mathbf{x}, t)$ to become n_0 than in (a). This also shows that the crossover in (b) occurs more slowly than in (a). In fact, from Fig. 2, ω_β in (b) is smaller than that in (a). Thus, the plateau height and the peak heights turn out to depend on how far from equilibrium the initial state is.

In order to see the time dependence of $F_S(\mathbf{k}, t)$ in terms of a power-law formula in the intermediate-time region, we also calculate the logarithmic derivative given by $\varphi = \partial \log[f_k^c - F_S(\mathbf{k}, t)] / \partial \log t$. Then, the effective exponent φ reveals two fairly plateau regions: $\varphi = b_0(\sigma, z_0)$ for $t_\gamma \ll t \ll t_\beta$ and $\varphi = b(\sigma, z_0)$ for $t_\beta \ll t \ll t_\alpha$, where the exponents b_0 and b are listed in Table I. For intermediate times, therefore, the relaxation proceeds in the following two time stages in the fluid

state ($\sigma < 0$): one is the so-called β -relaxation stage for $t_\gamma \ll t \ll t_\beta$ ($\omega_\beta \ll \omega \ll \omega_\gamma$), where the power laws hold

$$F_S^\beta(\mathbf{k}, t) = f_k^c - A_k(t/t_\beta)^{b_0}, \quad \chi_S''(\mathbf{k}, \omega) = A_k''(\omega/\omega_\beta)^{b_0}, \quad (11)$$

where A_k and A_k'' are weak functions of \mathbf{k} and σ . The other is the so-called α -relaxation stage for $t_\beta \ll t \ll t_\alpha$ ($\omega_\alpha \ll \omega \ll \omega_\beta$), where the power laws hold

$$F_S^\alpha(\mathbf{k}, t) = f_k^c - B_k(t/t_\alpha)^b, \quad \chi_S''(\mathbf{k}, \omega) = B_k''(\omega/\omega_\alpha)^{-b}, \quad (12)$$

where B_k and B_k'' are weak functions of \mathbf{k} and σ .

In conclusion, by solving the coupled diffusion equations numerically, we have shown how the initial inhomogeneities in space change the qualitative behavior of the relaxation processes near ϕ_g , leading to the two different slow relaxations. Such inhomogeneities start to become smooth, obeying the nonlinear deterministic equation (1). For regions where the number density $n(\mathbf{x}, t)$ is larger than the critical value $n_g = 3\phi_g/(4\pi a_0^3)$, however, the smoothing process is slowed down, leading to a structural arrest. Thus, the density fluctuations undergo a slow relaxation, although they are governed by the linear stochastic equation (2). The detailed analysis will be discussed elsewhere.

This work was supported by the Tohwa Institute for Science, Tohwa University.

-
- [1] P. N. Pusey and W. van Meegen, *Nature (London)* **320**, 340 (1986); *Phys. Rev. Lett.* **57**, 2083 (1987).
 [2] P. N. Pusey, in *Liquids, Freezing and the Glass Transition*, edited by D. Levesque, J. P. Hansen, and J. Zinn-Justin (Elsevier, Amsterdam, 1991).
 [3] W. van Meegen and S. M. Underwood, *Phys. Rev. E* **49**, 4206 (1994).
 [4] W. Götze and L. Sjögren, *Phys. Rev. A* **43**, 5442 (1991).
 [5] U. Bengtzelius, W. Götze, and A. Sjölander, *J. Phys. C* **17**,

5915 (1984).

- [6] M. Tokuyama and I. Oppenheim, *Phys. Rev. E* **50**, R16 (1994); *J. Korean Phys. Soc. Suppl.* **28**, S327 (1995); *Physica A* **216**, 85 (1995).
 [7] M. Tokuyama, *Physica A* **229**, 36 (1996).
 [8] M. Tokuyama, *Phys. Rev. E* **54**, R1062 (1996).
 [9] B. J. Berne and R. Pecora, *Dynamic Light Scattering* (Wiley, New York, 1976).